UCRL-53185

Nondestructive Evaluation of Electron-Beam Braze Joins

D. M. Boyd
J. F. Shackelford
B. W. Maxfield
G. M. Taylor

UCRL--53185
DE82 005846

August 18, 1981

Lawrence Livermore National Laboratory

Work performed under the auspices of the U.S. Department of Energy by Lawrence Livermore National Laboratory under Contract W-7405-Eng-48.

UCRL-53185
Distribution Category UC-38

Nondestructive Evaluation of Electron-Beam Braze Joins

D. M. Boyd

J. F. Shackelford

B. W. Maxfield

G. M. Taylor

Manuscript date: August 18, 1981

LAWRENCE LIVERMORE LABORATORY
University of California • Livermore, California • 94550

Available from: National Technical Information Service • U.S. Department of Commerce
5285 Port Royal Road • Springfield, VA 22161 • $5.00 per copy • (Microfiche $3.50)

Blank Page

CONTENTS

Nondestructive Evaluation of Electron Beam Braze Joins

ABSTRACT

A nondestructive evaluation (NDE) program has been carried out using holographic interferometry, microradiography, and eddy current testing for the inspection of electron beam braze joining of dissimilar metals. Stainless steel tubing was joined to a gold-copper disk using a Cusil (copper/silver) brazing alloy. Holographic interferometry provided an indirect measure of strength by detecting the plastic deformation occurring as a result of applying a stress. Microradiography with the aid of computer graphics displays provided a means of measuring braze penetration into the stainless steel tube. Correlation of results with metallographic examination and microhardness measurements show that holography and microradiography each provide quantitative braze quality rankings. Each method correctly identified variations in braze quality independent of electron beam power (the only processing variable in sample fabrication). Eddy current results were consistent with the other NDE methods but appear to be based on variation in surface topography rather than electrical conductivity. The usefulness of the eddy current method for this problem is questionable due to its sensitivity to the small, complex test piece geometry.

INTRODUCTION

Brazing is a means of joining similar or dissimilar metals by a "braze metal" that wets each of the joined surfaces.[1] The brazing temperature must be high enough to melt the braze material but low enough to prevent the heat input from destroying the mechanical or chemical properties of the joined metals. Factors that may influence electron beam brazing include beam diameter at the braze, beam position relative to the braze, and beam power. For these reasons it is often necessary to have a nondestructive evaluation procedure to ensure that the braze will perform adequately.[2]

This paper describes three nondestructive testing techniques used to evaluate an electron-beam-heated Cusil braze* joining a stainless steel tube to a work-hardened gold-copper alloy.[4,5] Six specimens were tested using holographic interferometry, microradiography, and eddy current measurements techniques. After sectioning the specimens, the results of the nondestructive tests were compared with photomicrographs of the sectional braze join, microhardness measurements of the heat-affected zone, and electron microprobe analysis of the braze material.

Our objective was to determine the influence of the electron beam input power used for brazing on the measurable properties of the braze. Microradiography[6] of the braze join, with the aid of computer graphics displays, was used to measure braze penetration into the stainless steel tube.[7] Double-exposure holographic interferometry was used to measure the plastic deformation that resulted around the braze join from the application of a stress.[8] The eddy current technique was used to measure variations in electrical conductivity of the braze region.

The results of this investigation showed there was a good correlation between the measurable parameters determined from the nondestructive testing and metallographic examination. It was also found that the input electron beam power affects the braze, but other beam parameters are also important.

*The nomenclature for this study acknowledges the use of a common brazing alloy (Cusil is 28 wt% Cu, 72 wt% Ag). It should be noted that the extent of melting occurring in the base metals is, in some cases, more characteristic of welding than brazing.[3]

SAMPLE PREPARATION

A 304 stainless steel tube, (1.0-mm o.d., 0.25-mm i.d.) was brazed to a flat disk (Au 5 wt% Cu alloy, 20-mm diam, 1-mm thick). The tubing was aligned over a 0.25-mm hole drilled through the center of the disk with the aid of a slightly recessed cavity in the disk surface large enough to accommodate the outside diameter of the tube. A 0.13-mm-diam ring of Cusil braze material was placed at the surface join between the two materials. The braze was melted by an electron beam (operating conditions approximately 60 kV and 3 mA) while the specimen was rotated in a holding fixture. A schematic of the final specimen configuration is shown in Fig. 1. Slight variations in beam current provided strong variation in braze character, namely from barely melted Cusil to heavily melted Cusil with attendent distortion of tube and disk geometry.

In the fabrication of these specimens, every effort was made to keep all parameters except the input power constant. In fact, there were probably other parameters which could affect braze characteristics that varied beyond the operator's control. Of particular importance may be the initial position and spot size of the electron beam.

The six specimens were put into three groups based on beam power input: "cold" (specimens F and G approximately 2.8 mA), "normal" (specimens C and D approximately 3.0 mA), and "hot" (specimens I and K approximately 3.2 mA). The hot, normal, and cold groupings were used for the qualitative nondestructive determination of the braze type.

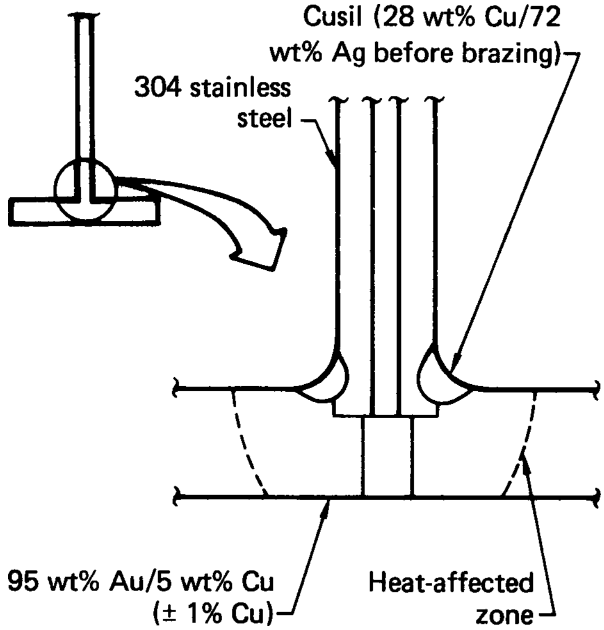

FIG. 1. **A schematic of a typical sample.**

TEST METHODS

HOLOGRAPHIC INTERFEROMETRY

Holographic evaluation of the braze join required stressing the disk sample. To provide a controlled application of the stress, a high pressure fitting was modified to secure the disk around the outer edge. The fitting allowed both viewing of the tube side of disk and controlled pressurization on the back side (see Fig. 2).

A coincident viewing and illumination holographic configuration[9] was used to measure the displacement caused by pressurization of the disk. All testing was performed in a modified high pressure cell designed for remote control holography.

The stress level for the disk tests was determined by calculating the pressure required for 50% of the known yield strength. A pressure of 10 MPa gives a maximum stress at the outer edge of 366 MPa, which is half the yield strength of this material.

Residual displacement holography was used during the testing of the six disks. The first exposure was made at a reference pressure of 1.7 MPa. The pressure was then brought up to the test pressure of 10 MPa and back to the reference pressure where a second exposure was made. The result was a holographic interferogram showing a contour map of the permanent residual displacement caused by the plastic deformation.

Six test cycles were run for each disk in increments of 0.7 MPa between 10.3 and 13.8 MPa.

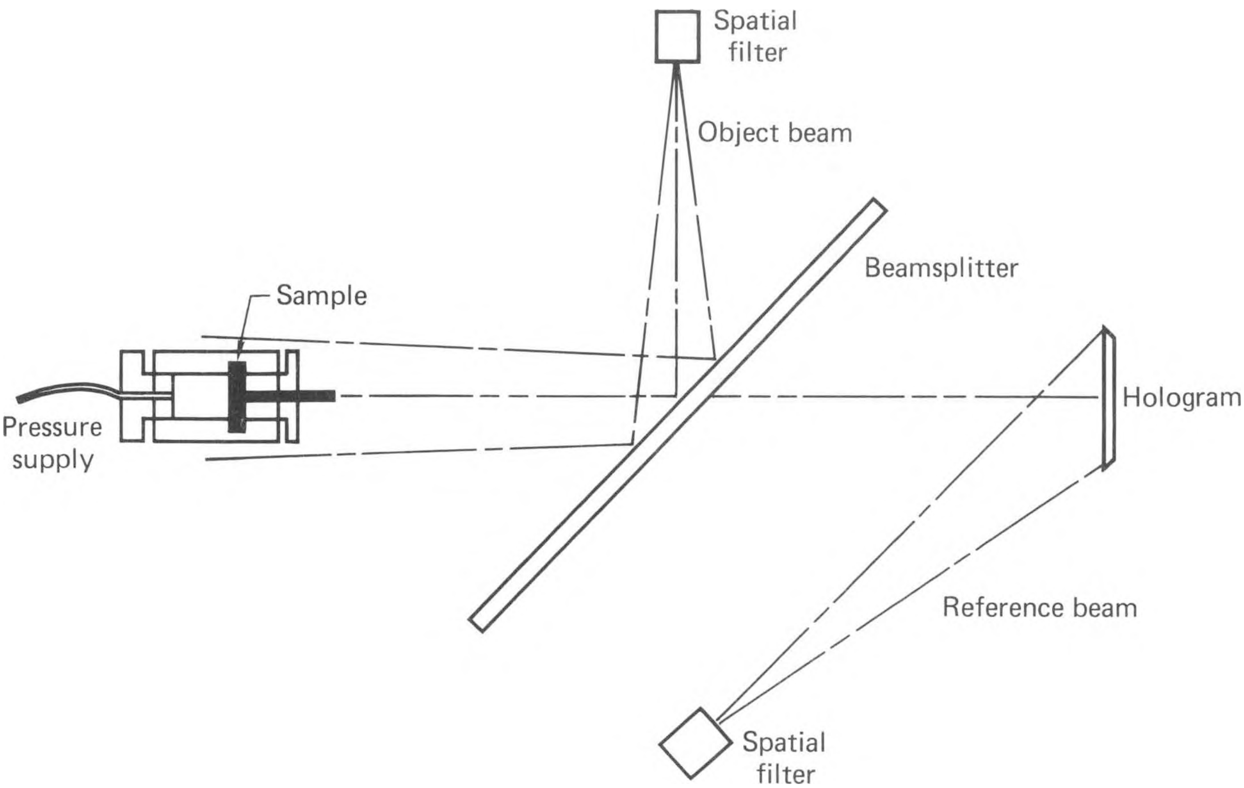

FIG. 2. Optical configuration used for double-exposure holographic testing.

MICRORADIOGRAPHY

An x-ray source operated at 150 kV and 4 mA was used for a 45-min exposure at 1.2 m (4 ft) source-to-film distance. A lead collimator was used to reduce scattering of the x-ray beam and a lead-oxide screen (approximately 0.1-mm thick) was used to enhance the quality of the final radiograph. Figure 3 shows a typical radiograph made with high-resolution photographic plates.

Interpretation of the radiographs was done with the aid of computer graphics displays of digitized film density measurements. Densitometer traces of the radiographic plates were made with a Photometric Data System (PDS) manufactured by Boller and Chivens (a subsidiary of Perkin and Elmer). The plate was scanned in 4-μm steps with a 4-μm aperture.

A 2500-by-2500-μm area centered on the join was scanned, giving 3.9×10^5 data points. A contour map of film densities was produced using the computer graphics code TRAX (available from the Technical Photography Department at Lawrence Livermore National Laboratory) and a CDC 7600 computer. Figure 4 shows a contour map of film densities in the area of the join corresponding to an enlargement of Fig. 3. The contour map outlines the area of the join.

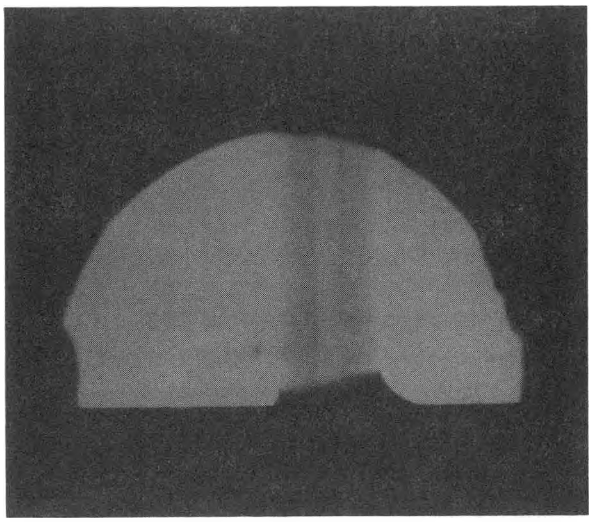

FIG. 3. Typical microradiograph.

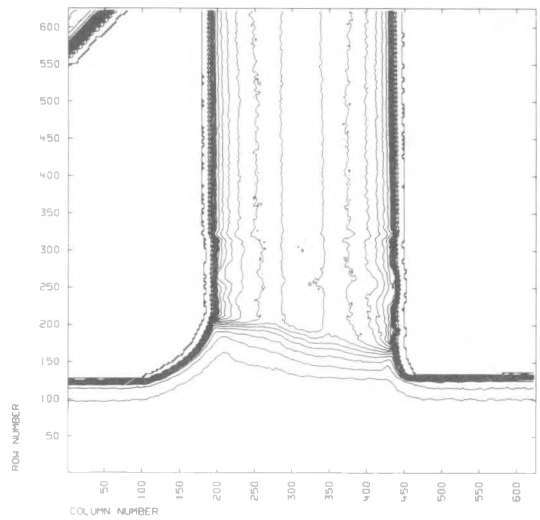

FIG. 4. Computer-generated contour map of microradiograph shown in Fig. 3.

Asymmetry of the braze around the tube surface required multiple-exposure angles. Each join was inspected from three equally spaced directions, as illustrated in Fig. 5.

EDDY CURRENTS

Variations in the welding parameters might be expected to result in variations in the composition of the metal in the immediate vicinity of the tube. These variations might, in turn, cause electrical conductivity changes which could be measured by an eddy current method. The effectiveness of such a method would depend on the degree of correlation between the measured eddy current values and the welding parameters. In addition, the eddy current response from this source would have to be separable from responses from other variables such as lift-off distance (related to local variations in geometry).

The heat-affected zone was so small that LLNL coils and equipment could not be used. A contract was made with the Reluxtrol Company in South San Francisco, Calif., to make some basic measurements on these specimens. Two special coils with the company designations of CREG 201 and CREG (a miniaturized probe) were used. The operating frequency chosen was 3 MHz. The instrument used is not specified in their report,[10] but apparently has an oscilloscope output that gives the

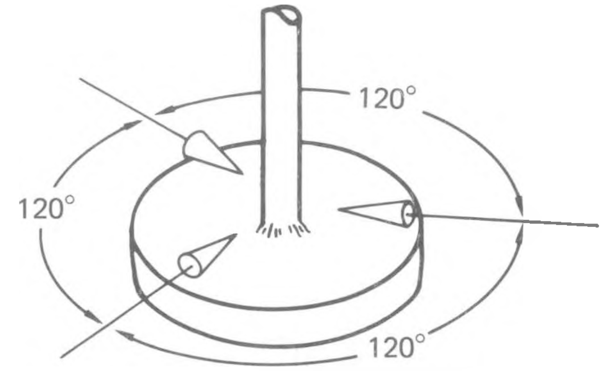

FIG. 5. Schematic of three-angle inspection orientation.

output voltage as two components at 90 electrical degrees with respect to each other. The phase of the output voltage could be rotated and was adjusted so that small changes in lift-off gave changes in a horizontal direction. The measurements were read in the vertical direction on the oscilloscope to reduce sensitivity to lift-off. The company's work is described in greater detail in Ref. 9.

After completion of the work under this contract, LLNL purchased a small coil from Reluxtrol and borrowed an instrument from Bendix in Kansas City, Mo., to make further measurements. The instrument was a Nortec Corp. NDT-15 modified to permit the coil and a reference coil to be attached. This instrument has an oscilloscope output, and two digital voltmeters were attached to read the horizontal and vertical component of voltage. The instrument would not balance at 3 MHz, so a frequency of 4.2 MHz was finally chosen.

The very small coil needed to resolve the area of interest was extremely sensitive to lift-off. A series of systematic measurements was made to determine this sensitivity and the coil's sensitivity to conductivity changes. In addition, the interaction of the coil's field in the direction of the tube was checked.

METALLOGRAPHY

Metallographic examination techniques were used to verify the results of the nondestructive measurements. Sectioning of the disks provided access to the braze area. Photomicrographs, microprobe analysis, and microhardness measurements were made on the sectioned specimens.

RESULTS

HOLOGRAPHIC INTERFEROMETRY

The residual displacement resulting from each of the pressure cycles is determined from the number of fringes around the tube. The optical configuration allows for easy conversion from fringes to displacement. Results for each of the test pressures for the six specimens are shown in Table 1. Samples I and K deformed so much that distinct holographic fringes were not discernable. A visual inspection of I and K showed obvious bowing of the disks.

Figure 6 shows typical holograms for samples C, D, G, and F from the test cycle to 12.4 MPa. The difference in residual displacement is attributed to the extent of the heat affected zone.

TABLE 1. Holographic residual displacement measurements of six disks (μm).

Max. Pressure (MPa)	Disk displacement (μm)					
	C	F	G	D	K	I
10.3	2.30	2.57	3.34	6.43/2.57	↑	↑
11.0	0.25	1.03	0.77	1.80		
11.7	0.51	0.51	1.80	0.25		
12.4	0.51	0.77	1.29	2.80		
13.1	0.51	0.51	1.80	3.09		
13.8	0.51	0.77	1.54	3.34		
Total displacement	4.54	6.16	10.54	20.28	Not measurable	

MICRORADIOGRAPHY

Figure 4 provides a useful visualization of the exterior geometry of the braze join. In order to quantify the interior geometry of the join, it is necessary to use another aspect of the computer graphics code. Figure 7 (a) shows a computer-generated plot of the film density for a horizontal scan of the tube. This is compared in Fig. 7 (b) with a calculated plot of the fraction of beam energy transmitted (I_x/I_0 from a simple Beer's law calculation) for a tube with similar geometry and composition. For the calculation, the effective beam energy from the 150-kV tube was assumed to be 100 keV. Because film density is a nonlinear function of beam intensity, the curves in Fig. 8 do not have the same form. However, the key feature is that there is a direct correlation between stem geometry (i.d. and o.d.) and sharp breaks in measured film density.

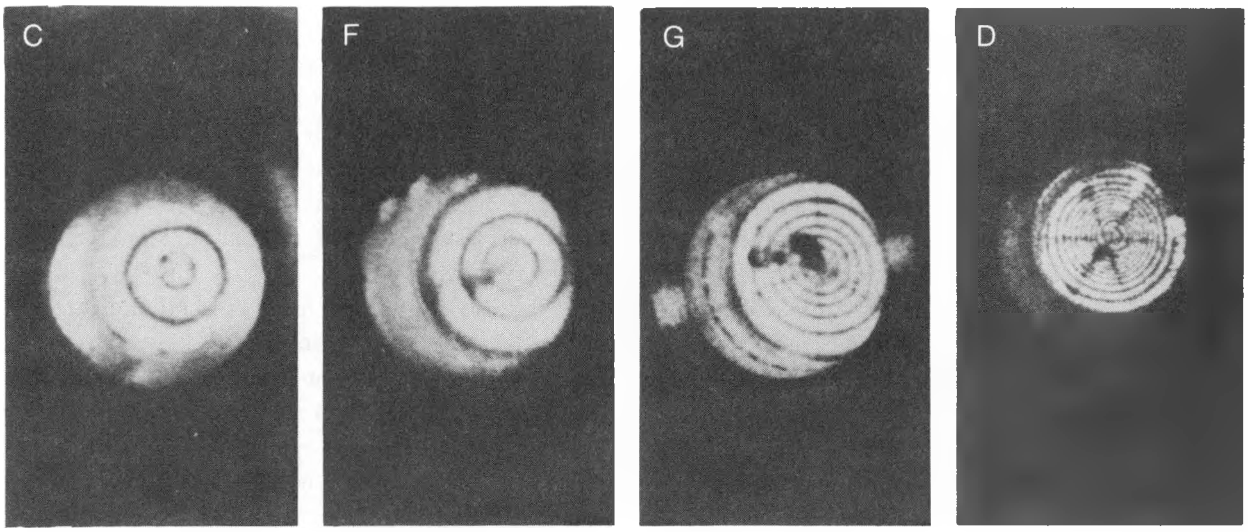

FIG. 6. Residual displacement fringe pattern at 12.4 MPa test pressure for samples C, F, G, and D.

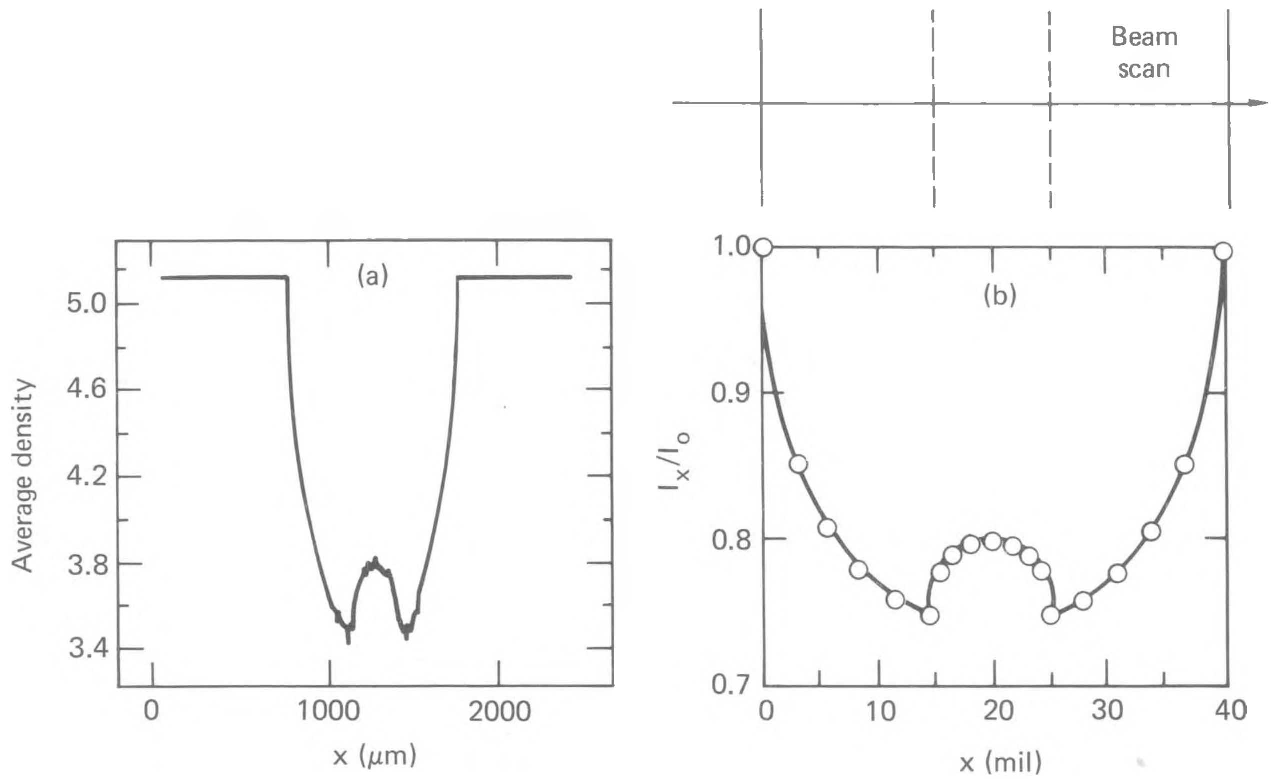

FIG. 7. (a) Experimental film density curve for tube. (b) Calculated x-ray attenuation curve for similar geometry and material.

Figure 8 shows a similar comparison of experiment and calculation for beam transmission through the braze.

Using the breaks in film density profiles to locate interior and exterior geometry, a braze intrusion map can be produced as shown in Fig. 9. A relatively precise identification of braze intrusion into the tube is possible. The production of a similar intrusion profile into the disk was not possible due to the high beam attenuation by the relatively large beam path through the high Z alloy.

Two parameters were used to characterize the extent of braze intrusion into the stem. Figure 10 defines the intrusion at half braze height (IHBH), which is a linear dimension, and the area of intrusion (AOI), which is a two-dimensional parameter.

Figure 11 summarizes typical braze intrusion maps for the three groups (hot, cold, and normal); the area of intrusion is shaded. The relative values of IHBH and AOI for the six specimens are shown in Table 2.

EDDY CURRENTS

The results obtained by Reluxtrol appeared to correlate well with the electron beam current used in the welding process (see Fig. 12). Subsequent measurements at LLNL, however, showed the great sensitivity of the coil to lift-off. The procedure used at Reluxtrol to decrease the effect of lift-off is adequate if the direction of the lift-off effect is constant or the magnitude sufficiently small so that no appreciable part of the measured signal change arises from that cause.

The measurements made at LLNL indicate that the lift-off effect may not have been minimized sufficiently. The structure of the braze metal was quite irregular in the immediate vicinity of the tube and the coil was placed on the surface when measurements were made. The result was that the effective distance of the metal "seen" by the coil varied appreciably around the tube and from sample to sample. The roughness of this contour also

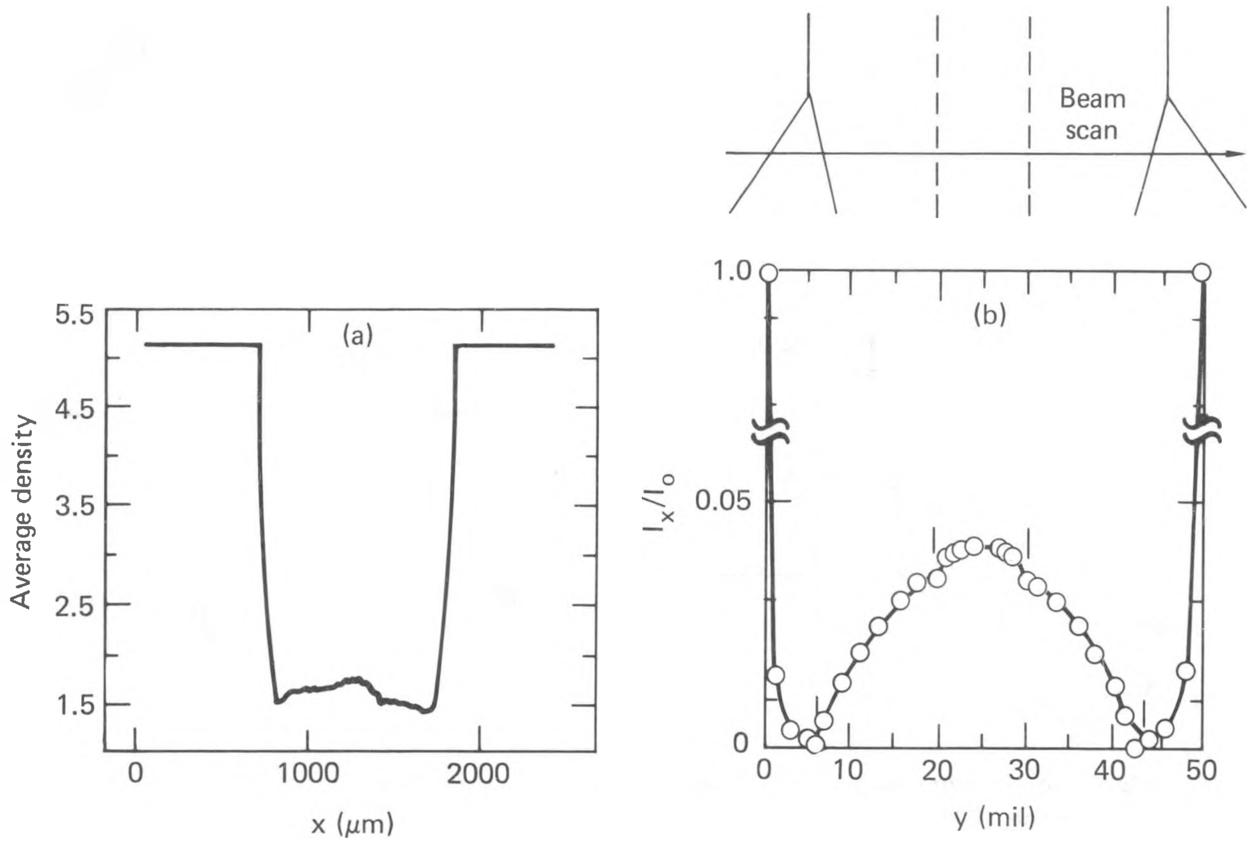

FIG. 8. (a) Experimental film density curve for braze join. (b) Calculated x-ray attenuation curve for similar geometry and material.

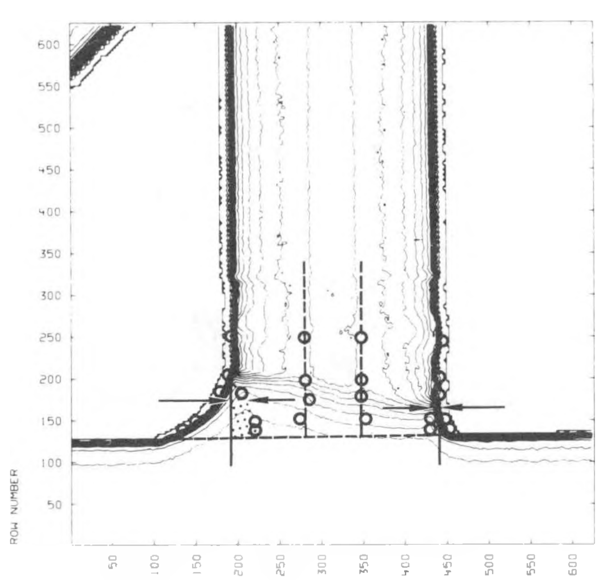

FIG. 9. Braze intrusion map for sample of Fig. 3.

correlated well with the heat input for the samples so the correlation between the eddy current results and brazing heat input may well have been the result of this factor rather than electrical conductivity.

METALLOGRAPHY

An indication of the braze intrusion into the disk is given by photomicrographs of Fig. 13. These show a greater depth of penetration into the lower melting point gold alloy than into the steel tube. Electron microprobe analysis showed that the braze pool became enriched with gold due to the melting of the disk alloy. The composition was fairly homogeneous with the gold content increasing with increasing degrees of disk melting. Gold content of well over 50 wt% was common in the braze pool.

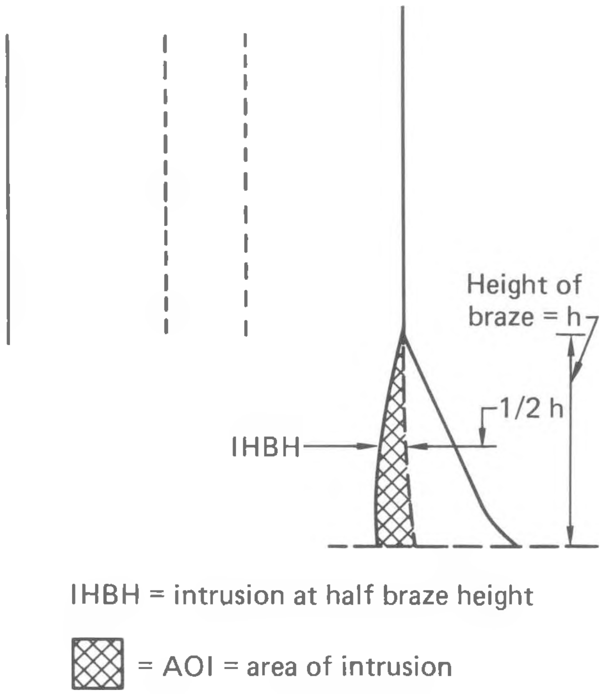

FIG. 10. Definition of intrusion at half braze height and area of intrusion.

TABLE 2. Braze intrusion in tube-disk joins.

Sample	IHBH[a] (μm)	AOI[a] (μm^2)
F	4	3×10^3
C	23	5×10^3
D	50	12×10^3
G	60	17×10^3
K	483	161×10^3
I	483	250×10^3

[a]Defined by FIG. 10.

Since much of the strength of the parent material comes from work-hardening, heating above the annealing point (which can result from the braze power input) will reduce the strength and hardness locally. For this reason, microhardness (spatial resolution about 0.5 mm) measurements were performed on all six specimens. All measurements were made along a radius extending from the center of the tube attachment to the edge of the disk. On each disk, two such sequences were made;

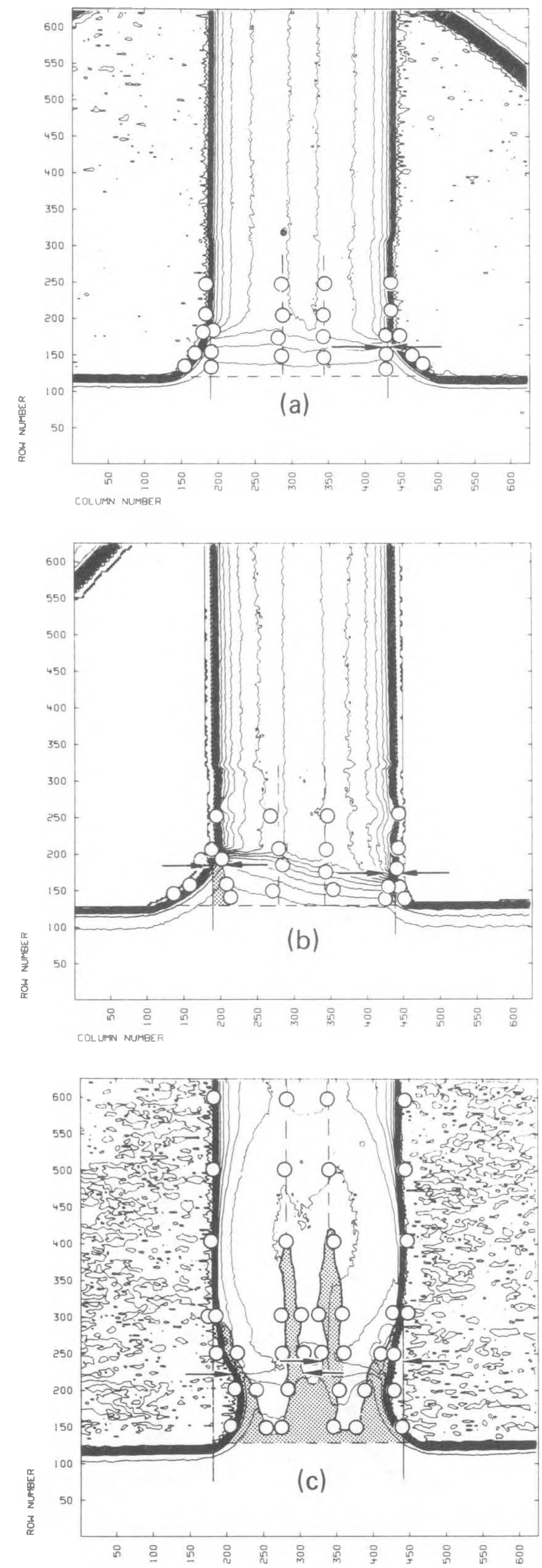

FIG. 11. Braze intrusion maps for typical (a) "low heat" braze, (b) "medium heat" braze, and (c) "high heat" braze.

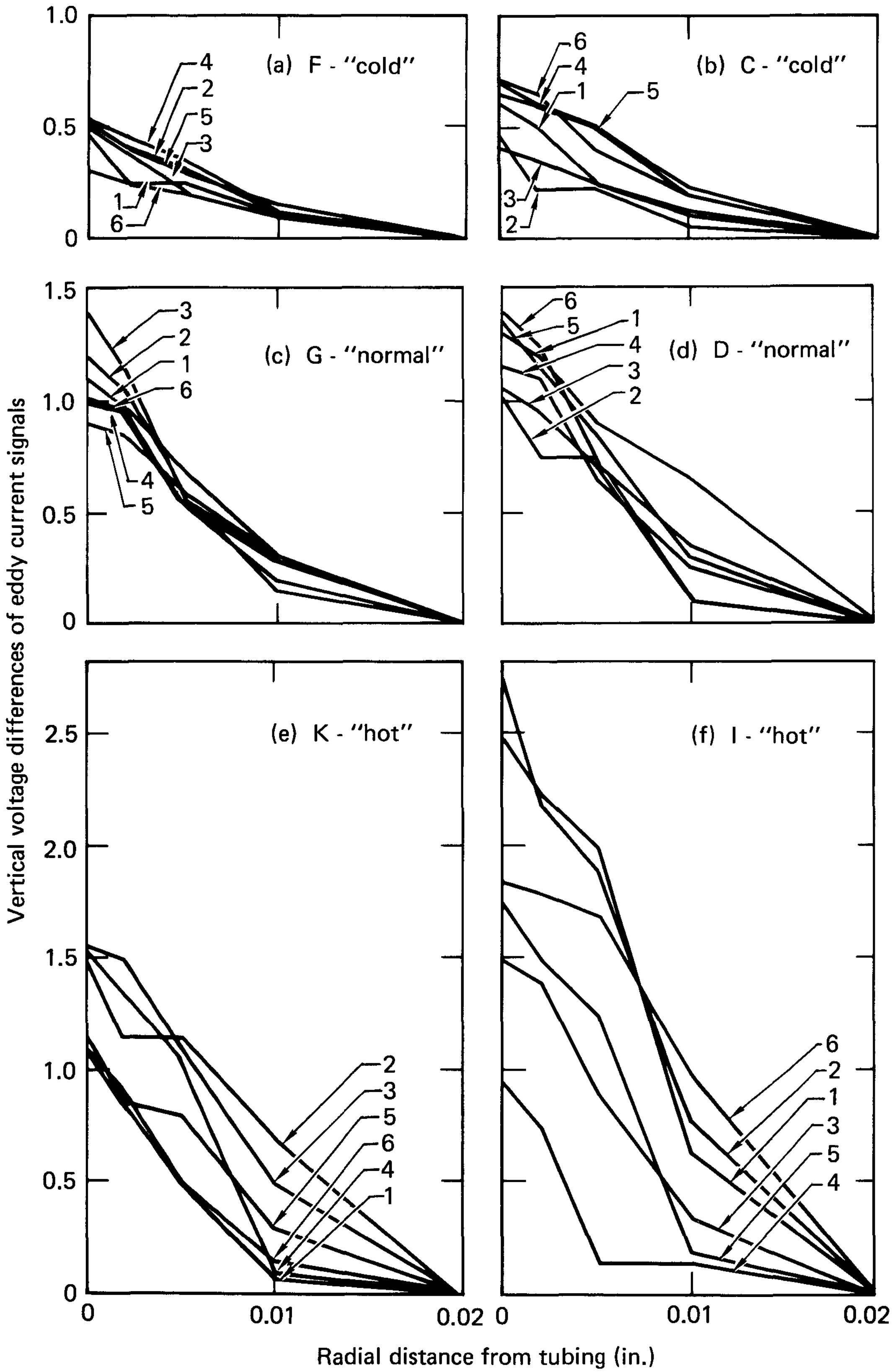

FIG. 12. Eddy current measurements along the radial distance from the tubing. Six radial measurements were made on each disk and are labeled 1 through 6.

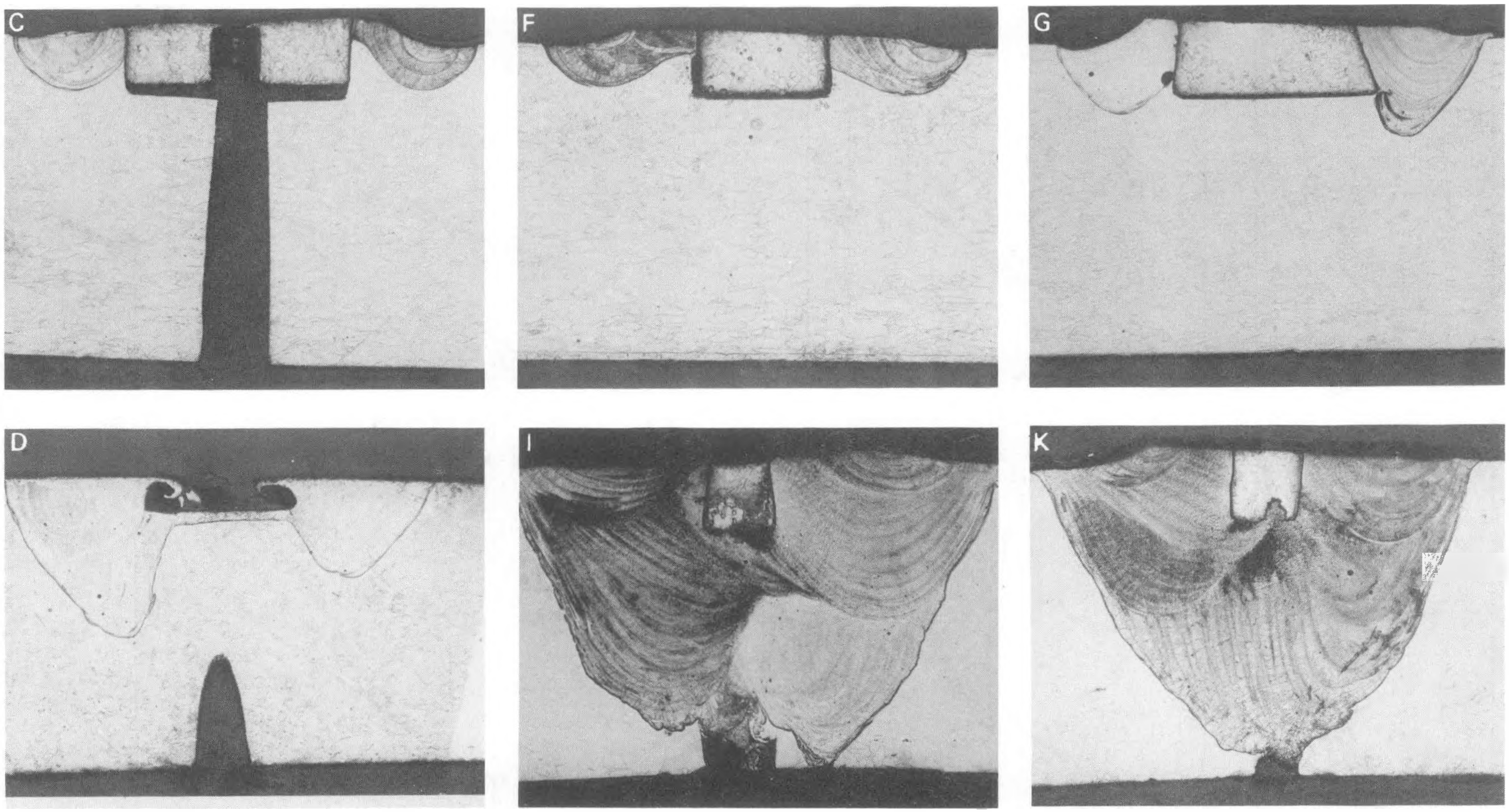

FIG. 13. Photomicrographs of six sectioned brazed joins (samples C, F, G, D, I, and K).

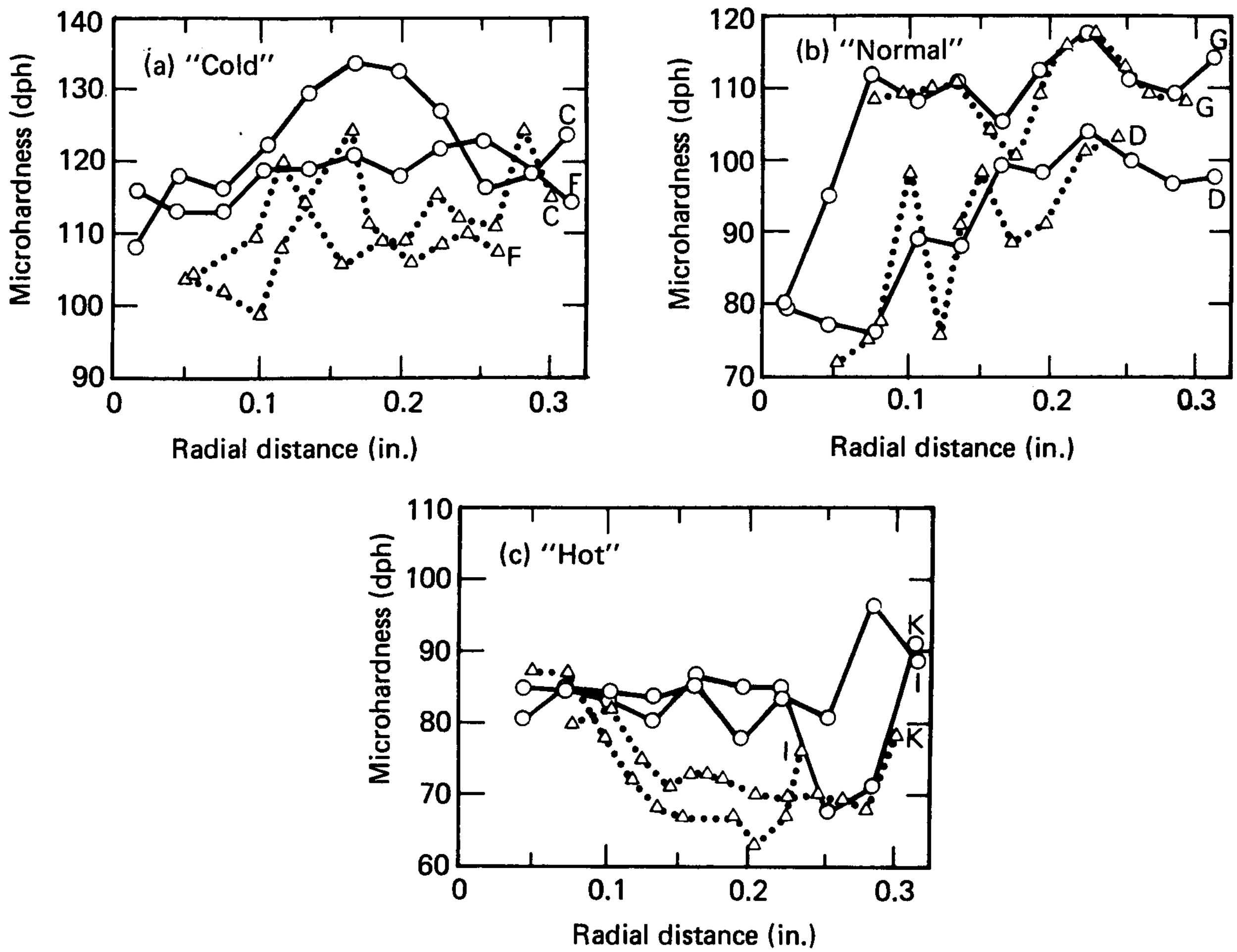

FIG. 14. Microhardness measurements along radius from braze pool. The circles are surface measurements and the triangles are sectioned measurements.

one along a line on the heated surface with results (Fig. 14) given by the circles connected with black lines and another midway through the disk with results given by the triangles connected with dotted lines. The former was done prior to sectioning and, obviously, the latter required sectioning the disk.

DISCUSSION

Six tube-disk joins were inspected. They were fabricated in three groups: a "normal heat" group (samples labeled C and D) produced with the standard electron beam current of 3 mA; a "low heat" group (F and G) with a beam current approximately 0.2 mA below standard; and a "high heat" group (I and K) with a beam current approximately 0.2 mA above standard. Table 3 summarizes the results of the nondestructive and metallographic inspections. It should be noted that specimens C and G are reversed based on the electron beam current. The complexity of the brazing process is such that the small current variations were not the only effect on final braze geometry. It should be noted that all measurements confirm that groupings F and C are low heat (penetration) specimens, D and G are normal, and K and I are high heat. However, the usefulness of an eddy current method for inspecting brazes of this type has not been fully established.

TABLE 3. **Summary of quantitative measurements made on electron beam braze.**

Method	Specimens		
	Cold	Normal	Hot
Holographic Interferometry	C F	G D	K I
Microradiography	F C	D G	K I
Eddy current	F C	G D	K I
Photomicrographs (area of braze pool)	C F	G D	K I
Microhardness	C F	G D	K I

The following conclusions may be drawn by comparing the signal changes that might be expected from an eddy current system as a result of changes in an alloy of the type considered here to the changes that might result from variations in lift-off. The surface flatness of the sample would have to be controlled to a very small tolerance and the shape would have to be uniform from part-to-part, or extremely accurate fixturing would be required to guarantee uniformity of test geometry. Also, the tube should be accurately positioned perpendicular to the surface. The eddy current technique also requires empirical standards for calibration, and measurement of both components of the eddy current signal.

CONCLUSION

For brazes made under nearly identical conditions except for the electron-beam input power, the techniques of holographic interferometry and microradiography were able to make quantitative rankings of the braze quality.* The results of the nondestructive techniques were verified by the metallographic examination and the microhardness measurements. The results also showed that input beam power is not the only parameter that affects the braze.

The nondestructive techniques of holography and microradiography were shown to be valuable in braze evaluations. The residual displacement holography technique provides an indirect measure of the strength by detecting the plastic deformation occurring as a result of applying a stress. Microradiography with the aid of computer graphics displays provided a means of measuring braze penetration into the stainless steel tube. This test shows that either technique could be used as a nondestructive method of measuring component serviceability.

ACKNOWLEDGMENTS

A. J. Schwarber supervised all microradiographic testing by the technical staff of the Nondestructive Evaluation (NDE) Section at Lawrence Livermore National Laboratory. Claude Dittmore performed the scanning densitometry of the microradiographs. David H. Wood, David Diaz, and Wayne Steele provided metallographic and electron microprobe inspections. William Wilcox and Linwood Hester performed the holographic pressure tests.

*The eddy current results also indicated the ability to rank the braze quality; however, these measurements appeared to be affected by variation in surface topography and not the change in electrical conductivity of the braze pool.

REFERENCES

1. *Brazing Manual,* (AWS Committee on Brazing and Soldering, American Welding Society, Inc., 1976), 3rd ed. pp. 155–159.
2. R. Bakish and S. S. White, *Handbook of Electron Beam Welding* (John Wiley and Sons Inc., New York, 1964), pp. 247–249.
3. *Metals Handbook,* T. Lyman, Ed. (American Society for Metals, Metals Park, OH, 1961), 8th ed. vol. 1, pp. 5, 40.
4. J. H. Smith and M. B. Bever, "Stored Energy, Electrical Resistivity, and Tensile Properties of Cold-Worked Gold," in *Trans. AIME* **242**, 880 (1968).
5. D. E. Lord and L. F. Meisner, *A Cryoforming Evaluation Using Gold-5% Copper,* Lawrence Livermore National Laboratory, Livermore, CA, UCID-17281 (1976).
6. *Nondestructive Testing Handbook,* R. C. McMaster, Ed. (Ronald Press, New York, N.Y., 1963), sec. 20, pp. 41–45.
7. J. F. Shackelford, *Microradiography of Electron Beam Braze Joins,* Lawrence Livermore National Laboratory, Livermore, CA, UCID-18813 (1980).
8. D. M. Boyd, "Holographic Interferometry Applied to Braze Evaluations," in *Proc. Topical Meeting on Hologram Interferometry and Speckle Metrology,* Optical Society of America, N. Falmouth, Mass. June 2–4, 1980.
9. L. O. Heflinger, R. F. Wuerker, and H. A. Spetzler, "Thermal Expansion Measurements of Diffusely Reflecting Samples by Holographic Interferometry," in *Rev. Sci. Instr.* **44,** 629 (1973).
10. The Reluxtrol Company, "Measurement of Cusil Profile with Focused CREG Eddy Current Probes," LLNL Contract 652710937.

RMD/ig

LLNL* 1981/12